

An inspection of the runoff of an electrochemical grinding process using a constant voltage and a constant feed rate.

TABLE OF CONTENTS

1. OBJECTIVE.....	4
2. INTRODUCTION	4
2.1. LIST OF SYMBOLS.....	4
2.2. EQUATIONS USED.....	5
2.2.1. VOLUMETRIC REMOVAL RATE ACCORDING TO FARADAY [1].....	5
2.2.2. MASS REMOVAL RATE ACCORDING TO FARADAY.....	5
2.2.3. ELECTROCHEMICAL EQUIVALENT	5
2.2.4. PROCESS TIME.....	5
2.2.5. MACHINED VOLUME	5
2.2.6. ACTUAL VOLUMETRIC REMOVAL RATE (FROM DEPTH DATA).....	5
2.2.7. ACTUAL VOLUMETRIC REMOVAL RATE (FROM WEIGHT DATA).....	5
3. EXPERIMENTAL APPARATUS	7
3.1. MODIFIED PLANE GRINDING MACHINE	7
3.2. LABORATORY POWER SUPPLY.....	8
3.3. CONDUCTIVITY METER.....	8
4. EXPERIMENTAL PROCEDURE	8
5. PRESENTATION OF RESULTS.....	9
5.1. VOLUMETRIC REMOVAL RATE ACCORDING TO FARADAY [1]	9
5.2. MASS REMOVAL RATE ACCORDING TO FARADAY.....	9
5.3. ELECTROCHEMICAL EQUIVALENT.....	10
5.4. PROCESS TIME	10
5.5. MACHINED VOLUME.....	12
5.6. ACTUAL VOLUMETRIC REMOVAL RATE (FROM DEPTH DATA)	12
5.7. ACTUAL VOLUMETRIC REMOVAL RATE (FROM WEIGHT DATA).....	13
6. DISCUSSION OF RESULTS.....	15
7. CONCLUSION	16
8. REFERENCES.....	16
9. APPENDIX.....	17

LIST OF TABLES

TABLE 1 - LIST OF SYMBOLS.....	4
TABLE 2 - CINCINNATI MODIFIED PLANE GRINDER WITH ACCESSORIES.....	7
TABLE 3 - LABORATORY POWER SUPPLY SPECIFICATIONS.....	8
TABLE 4 - CONDUCTIVITY METER SPECIFICATIONS.....	8
TABLE 5 - 304 TYPE STAINLESS STEEL COMPOSITION.....	8
TABLE 6 - ELECTROLYTE PROPERTIES.....	8
TABLE 7 - RECORDED DATA.....	17

TABLE OF FIGURES

FIGURE 1 - ECG CATEGORISATION	6
FIGURE 2 - ECG PROCESS COMPONENTS.....	6
FIGURE 3 - SCHEMATICS OF SURFACE GRINDING IN ECG [1].....	6
FIGURE 4 - ECG MA+ECD.....	6
FIGURE 5 - ECG MACHINING SYSTEM COMPONENTS.....	6
FIGURE 6 - LABORATORY POWER SUPPLY PS9080.....	8
FIGURE 7 - VRR ACC. TO FARADAY, $U=CONST.$, $F\neq CONST.$	9
FIGURE 8 - VRR ACC. TO FARADAY, $U\neq CONST.$, $F=CONST.$	9
FIGURE 9 - MRR ACC. TO FARADAY, $U=CONST.$, $F\neq CONST.$	9
FIGURE 10 - MRR ACC. TO FARADAY, $U\neq CONST.$, $F=CONST.$	9
FIGURE 11 - MACHINING TIME VERSUS FEED RATE, $U=CONST.$, $F\neq CONST.$	11
FIGURE 12 - MACHINING TIME VERSUS FEED RATE, $U\neq CONST.$, $F=CONST.$	11
FIGURE 13 - MACHINED VOLUME VERSUS FINAL DEPTH OF CUT, $U=CONST.$, $F\neq CONST.$	12
FIGURE 14 - MACHINED VOLUME VERSUS FINAL DEPTH OF CUT, $U\neq CONST.$, $F=CONST.$	12
FIGURE 15 - ACTUAL VRR (DEPTH DATA) VERSUS MACHINING TIME, $U=CONST.$, $F\neq CONST.$	12
FIGURE 16 - ACTUAL VRR (DEPTH DATA) VERSUS MACHINING TIME, $U\neq CONST.$, $F=CONST.$	12
FIGURE 17 - ACTUAL VRR (DEPTH DATA) VERSUS WEIGHT LOSS / UNIT TIME, $U=CONST.$, $F\neq CONST.$	13
FIGURE 18 - ACTUAL VRR (DEPTH DATA) VERSUS WEIGHT LOSS / UNIT TIME, $U\neq CONST.$, $F=CONST.$	13
FIGURE 19 - SURFACE FINISH VERSUS FEED RATE, $U=CONST.$	13
FIGURE 20 - SURFACE FINISH VERSUS FEED RATE, $U\neq CONST.$ [2].....	13
FIGURE 21 - CURRENT VERSUS FEED RATE.....	13
FIGURE 22 - CURRENT VERSUS VOLTAGE.....	13
FIGURE 23 - FEED RATE VERSUS MRR ACCORDING TO FARADAY, $U=CONST.$	14
FIGURE 24 - VOLTAGE VERSUS MRR ACCORDING TO FARADAY, $U=CONST.$	14
FIGURE 25 - VOLUMETRIC REMOVAL RATES VERSUS VOLTAGE, $F=CONST.$	14
FIGURE 26 - VOLUMETRIC REMOVAL RATES VERSUS FEED RATE, $U=CONST.$	14
FIGURE 27 - MASS REMOVAL RATE ACCORDING TO FARADAY VERSUS CURRENT, $U=CONST.$	14
FIGURE 28 - MASS REMOVAL RATE ACCORDING TO FARADAY VERSUS CURRENT, $F=CONST.$	14
FIGURE 29 - CURRENT VERSUS VOLTAGE, $F=CONST.$ (AT $I=0$, ΔV IS THE OVERPOTENTIAL).....	15

1. OBJECTIVE

The objective of this experiment was to inspect the runoff of an electrochemical grinding process and to examine the results at a constant voltage and a constant feed rate. Utilising the experiment data, it is expected that relevant information concerning the relationship between process parameters, such as feed rate, voltage, current, surface finish and material removal rate will be made available.

2. INTRODUCTION

The experiment was carried out on a modified plane grinding machine. The diamond-grit coated rotating steel tool proceeded with the process at a previously set feed rate above the plane of the surface to be machined with predefined electrical parameters for each experimental setup. The component machined under the constant flow of an electrolyte was a stainless steel prismatic bar.

2.1. LIST OF SYMBOLS

Table 1 - List of symbols

SYMBOL	UNIT	DESCRIPTION
a	$\left[\frac{g}{mol}\right]$	Atomic weight of the anode metal
a_p	$[mm]$	Depth of cut
E	$\left[\frac{g}{C}\right]$	Electrochemical equivalent
f	$\left[\frac{mm}{s}\right]$	Feed rate
F	$[C]$	Faraday constant
I	$[A]$	Current
l	$[mm]$	Length of the component
m	$[g]$	Mass of the component
\dot{m}_D	$\left[\frac{g}{min}\right]$	Mass removal rate (Faraday)
Δm	$[g]$	Change of mass of the work piece
ρ	$\left[\frac{g}{cm^3}\right]$	Density of the work piece
t	$[min]$	Machining time
V_m	$[mm^3]$	Machined volume
\dot{V}_D	$\left[\frac{g}{mol}\right]$	Volumetric removal rate (depth data)
\dot{V}_F	$\left[\frac{g}{mol}\right]$	Volumetric removal rate (Faraday)
\dot{V}_w	$\left[\frac{g}{mol}\right]$	Volumetric removal rate (weight data)
w	$\left[\frac{g}{mol}\right]$	Width of the component
z	$[-]$	Valency of the anode metal

2.2. EQUATIONS USED

2.2.1. VOLUMETRIC REMOVAL RATE ACCORDING TO FARADAY [1]

$$\dot{V}_F = \frac{a \cdot I}{z \cdot F \cdot \rho} \cdot 60 \cdot 1000 \quad \left[\frac{\text{mm}^3}{\text{min}} \right] \quad (1)$$

2.2.2. MASS REMOVAL RATE ACCORDING TO FARADAY

$$\dot{m}_D = E \cdot I \cdot 60 \quad \left[\frac{\text{g}}{\text{min}} \right] \quad (2)$$

2.2.3. ELECTROCHEMICAL EQUIVALENT

$$E = \frac{a/z}{F} \quad \left[\frac{\text{g}}{\text{C}} \right] \quad (3)$$

Because the stainless steel is a heavily alloyed steel, the $\frac{a}{z} = \varepsilon$ (atomic weight equivalent) needs to be calculated in the following manner:

$$\varepsilon_{\text{ALLOY}} = \frac{100}{\sum_1^n \frac{xz}{a}} \quad \left[\frac{\text{g}}{\text{C}} \right] \quad (3.1)$$

where x is the percentage by weight of the component

2.2.4. PROCESS TIME

$$t = \frac{l}{f} \cdot 60 \quad [\text{min}] \quad (4)$$

2.2.5. MACHINED VOLUME

$$V = I \cdot w \cdot d_f \quad [\text{mm}^3] \quad (5)$$

2.2.6. ACTUAL VOLUMETRIC REMOVAL RATE (FROM DEPTH DATA)

$$\dot{V}_D = \frac{V}{t} \quad \left[\frac{\text{mm}^3}{\text{min}} \right] \quad (6)$$

2.2.7. ACTUAL VOLUMETRIC REMOVAL RATE (FROM WEIGHT DATA)

$$\dot{V}_W = \frac{\Delta m}{\rho \cdot t} \quad \left[\frac{\text{mm}^3}{\text{min}} \right] \quad (7)$$

The electrochemical grinding process (ECG) is a subset of the machining family known as electrochemical machining (ECM). According to [1], it can be categorised as a hybrid ECM process because of the presence of mechanical abrasion (MA) next to the electrochemical dissolution (ECD) as seen in Fig. 1-2. It utilises a negatively charged abrasive grinding wheel, which works on a positively charged work piece while being flooded with an electrolyte solution in a closed circuit system. Unlike ECM, the cathode is a specially constructed grinding wheel instead of a tool shaped like the contour to be machined. The insulating abrasive material (diamond or aluminium-oxide) on the grinding wheel is brought onto the wheel with the help of a conductive material. In this way, the non-conductive particles act as a spacer between the conductive material on the grinding wheel and the work piece.

According to [1], a constant inter-electrode gap can be maintained (0.025 mm) through which the electrolyte flood can be maintained. The schematics of a general surface grinding setup can be seen in Figure 3-4.

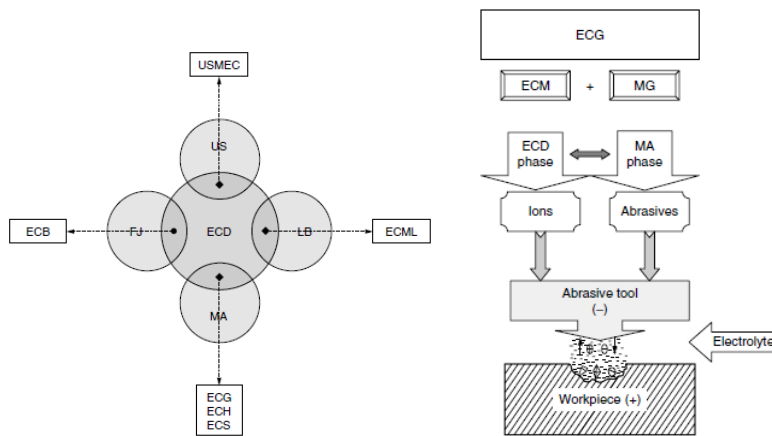


Figure 1 - ECG categorization

Figure 2 - ECG process components

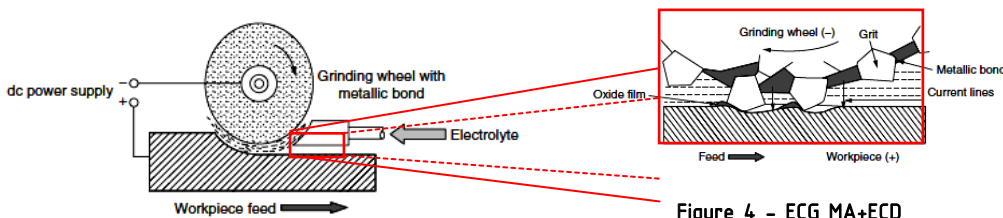


Figure 4 - ECG MA+ECD

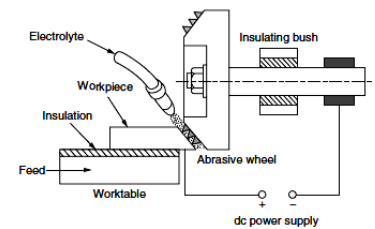


Figure 5 - ECG machining system components

The abrasive particles continuously remove the machining products from the work area. In the machining system shown in Fig. 5, the wheel is a rotating cathodic tool with abrasive particles (usually 60–320 grit number) on its surface. For ECD, electrolyte flow, usually NaNO_3 , is provided. The wheel rotates at a surface speed of 20 to 35 m/s, while current ratings are from 50 to 300 A.

The introduction of MA enhances the ECD process. The coated grinder wheel performs the mechanical abrasion of the possible insoluble film from the anodic work piece surface. Such films are formed especially when there are alloys of many metals and cemented carbides.

There are four process modes available for use with ECG: total mechanical removal (I), combined mechanical and electrolytic (II & III depending on the ratio of MA and ECD) and total electrolytic removal (IV).

Advantages:

- easy machinability of Ti-alloys (and other hard metals)
- absence of work hardening
- no grinding burrs
- good surface quality
- absence of distortion in thin/fragile/thermosensitive parts
- production of narrow tolerances
- longer grinding wheel life
- high material removal rate
- relatively small environmental impact, because of the reuse of the electrolyte
- economically viable machining of high grade aerospace components made possible

Disadvantages:

- initial implementation costs are high
- the process is limited to electrically conductive materials

3. EXPERIMENTAL APPARATUS

3.1. MODIFIED PLANE GRINDING MACHINE

For the experiment, a modified plane grinding machine was used. The changes include:

- the introduction of an electrolyte circulation system with a pump and filters
- the modification of the feed mechanism with the help of a proactive hydraulic and a counteractive pneumatic cylinder
- work enclosure mounted to prevent fluid from spilling
- the installation of a residual gas (Hydrogen) extraction system and a sludge removal unit
- tank for the electrolyte
- as an accessory unit, an electric amplifier was used for controlling the DC


Table 2 - Cincinnati modified plane grinder with accessories

PARAMETER	VALUE	IMAGE
Manufacturer	Cincinnati	
Worktable movement range X,Y,Z	N/A	
Positioning accuracy	N/A	
TOOL		
Grit type	diamond	
Mesh size	100/120	
Width	12.7 mm	
Layer thickness	0.152 mm	
Grit protrusion	0.025 - 0.05	
	ELECTROLYTE CIRCULATION SYSTEM	
	WORK ENCLOSURE	
	HYDRAULIC CYLINDER	
	PNEUMATIC CYLINDER	




3.2. LABORATORY POWER SUPPLY

Table 3 - Laboratory power supply specifications

PARAMETER	VALUE	IMAGE
Manufacturer	Elektro-Automatik GmbH & Co. KG	 <p>Figure 6 - Laboratory power supply PS9080</p>
Model number	PS9080 - 100 2HE	
Voltage range	0-80 V	
Current range	0-100 A	
Power	3000 W	

3.3. CONDUCTIVITY METER

Table 4 - Conductivity meter specifications

PARAMETER	VALUE	IMAGE
Manufacturer	Portland Electronics	
Model number	P335	

4. EXPERIMENTAL PROCEDURE

The stainless steel was mounted on the ECG machine worktable with the help of a magnetic work holder. It was aligned parallel with the side plane of the grinding wheel.

Table 5 - 304 Type stainless steel composition

DIN notation	EN	SAE	UNS	% Cr	% Ni	% C	% Mn	% Si	% P	% S	% N	Other
1,4301	X5CrNi18-10	304	S30400	18-20	8-10,50	0,08	2	0,75	0,045	0,03	0,1	-

The experiment was divided into two parts. In the first part, the bar was machined at a constant voltage, with varying feed rate. In the second part, the feed rate was kept constant, and the voltage varied.

After the aeration system was turned on, the sodium-nitrate electrolyte flow was initiated. Both systems were on for the full time of the machining sequence.

Table 6 - Electrolyte properties

NAME	COMPOSITION	m/m	APPEARANCE	PHYSICAL	ODOR	pH	CONDUCTIVITY (K)	FLOW RATE
------	-------------	-----	------------	----------	------	----	------------------	-----------

		[%]		STATE			[1/Ωmm]	[l/s]
Sodium-nitrate aqueous solution	NaNO ₃	10	clear, colorless	liquid	odorless	-9	0.011	0.114

A DC current was then switched on the machine, and the feeding was started. The regulation and the accuracy of the feed mechanism were ensured by the coupling of a pneumatic and a hydraulic piston to produce the necessary feed. The process was then conducted according to the two steps mentioned earlier.

5. PRESENTATION OF RESULTS

5.1. VOLUMETRIC REMOVAL RATE ACCORDING TO FARADAY [1]

$$\dot{V}_F = \frac{a \cdot I}{z \cdot F \cdot \rho} \cdot 60 \left[\frac{mm^3}{min} \right] \quad (1)$$

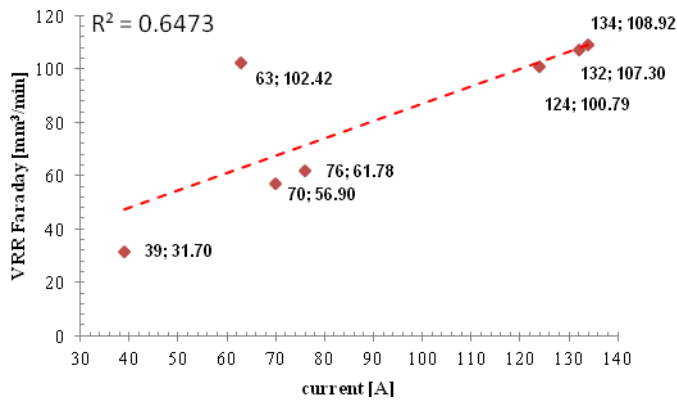


Figure 7 - VRR acc. to Faraday, U=const., f≠const.

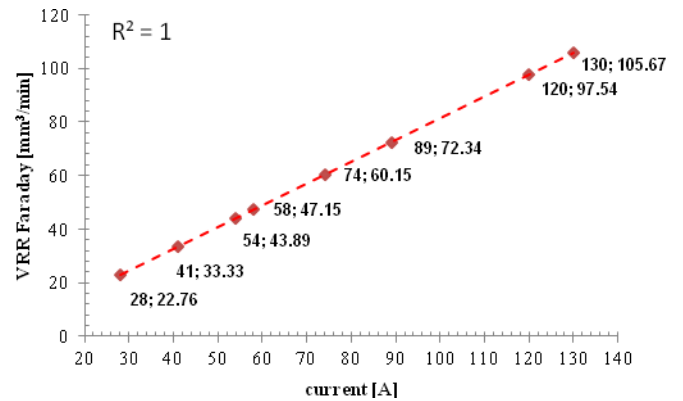


Figure 8 - VRR acc. to Faraday, U≠const., f=const.

5.2. MASS REMOVAL RATE ACCORDING TO FARADAY

$$\dot{m}_D = E \cdot I \cdot 60 \left[\frac{g}{min} \right] \quad (2)$$

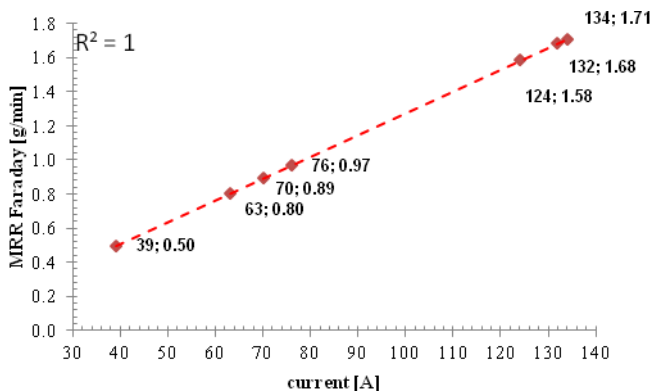


Figure 9 - MRR acc. to Faraday, U=const., f≠const.

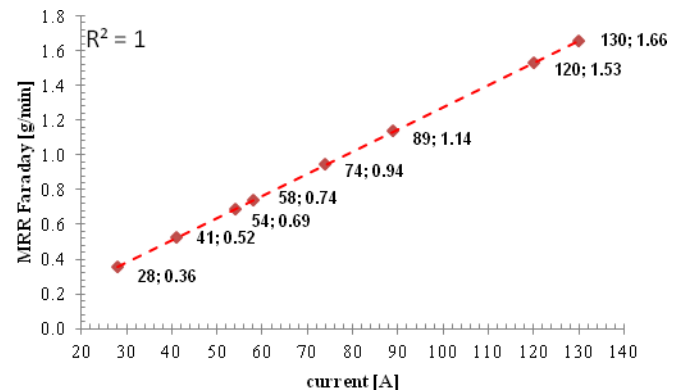


Figure 10 - MRR acc. to Faraday, U≠const., f=const.

5.3. ELECTROCHEMICAL EQUIVALENT

$$E = \frac{a}{z} \left[\frac{g}{C} \right] \quad (3)$$

$$E = 2.127 \cdot 10^{-4} \frac{g}{C}$$

Because the stainless steel is a heavily alloyed steel, the $\frac{a}{z} = \varepsilon$ (atomic weight equivalent) needs to be calculated in the following manner for the chemical composition previously mentioned:

$$\varepsilon_{ALLOY} = \frac{100}{\sum_1^n \frac{xZ}{a}} \left[\frac{g}{C} \right] \quad (4)$$

$$\begin{aligned} \varepsilon_{ALLOY} &= \frac{100}{\sum \left(\frac{z_{Cr} \cdot x_{Cr}}{a_{Cr}} + \frac{z_{Ni} \cdot x_{Ni}}{a_{Ni}} + \frac{z_C \cdot x_C}{a_C} + \frac{z_{Mn} \cdot x_{Mn}}{a_{Mn}} + \frac{z_{Si} \cdot x_{Si}}{a_{Si}} + \frac{z_P \cdot x_P}{a_P} + \frac{z_S \cdot x_S}{a_S} + \frac{z_N \cdot x_N}{a_N} + \frac{z_{Fe} \cdot x_{Fe}}{a_{Fe}} \right)} = \\ &= \frac{100}{\sum \left(\frac{19\% \cdot 2}{52} + \frac{9\% \cdot 2}{59} + \frac{0.08\% \cdot 4}{12} + \frac{2\% \cdot 2}{55} + \frac{0.075\% \cdot 4}{28} + \frac{0.045\% \cdot 5}{31} + \frac{0.03\% \cdot 2}{32} + \frac{0.1\% \cdot 3}{14} + \frac{68.995\% \cdot 3}{56} \right)} \end{aligned}$$

$$\frac{a}{z} = \varepsilon_{ALLOY} = 20.522 [g]$$

where x is the percentage by weight of the component

5.4. PROCESS TIME

$$t = \frac{l}{60 \cdot f} \quad [min] \quad (5)$$

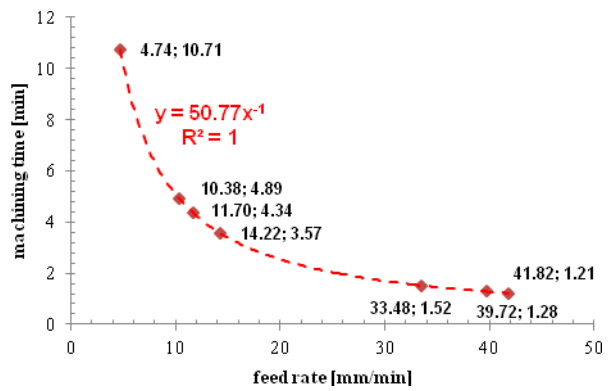


Figure 11 - Machining time versus feed rate, $U=\text{const.}$, $f \neq \text{const.}$

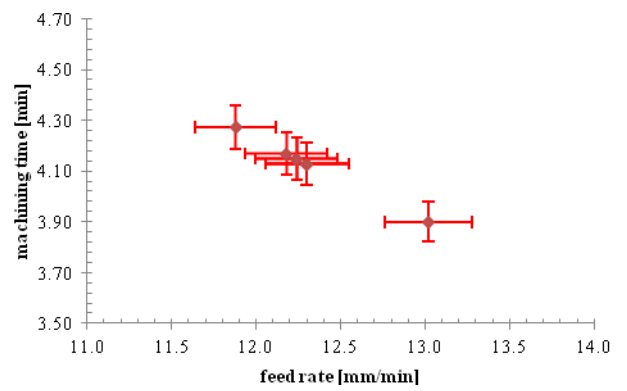


Figure 12 - Machining time versus feed rate, $U \neq \text{const.}$, $f = \text{const.}$

5.5. MACHINED VOLUME

$$V_m = l \cdot w \cdot a_p \quad [mm^3] \quad (6)$$

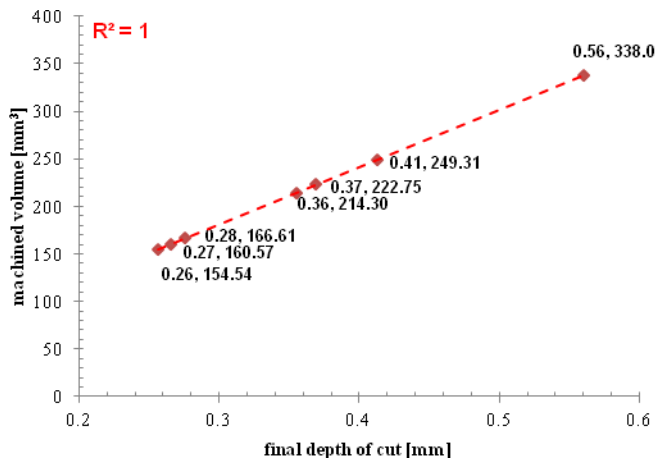


Figure 13 - Machined volume versus final depth of cut, $U=const.$, $f \neq const.$

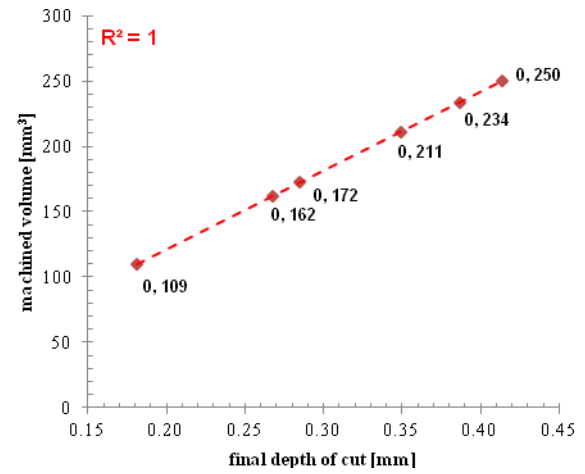


Figure 14 - Machined volume versus final depth of cut, $U \neq const.$, $f=const.$

5.6. ACTUAL VOLUMETRIC REMOVAL RATE (FROM DEPTH DATA)

$$\dot{V}_D = \frac{V}{t} \quad \left[\frac{mm^3}{min} \right] \quad (7)$$

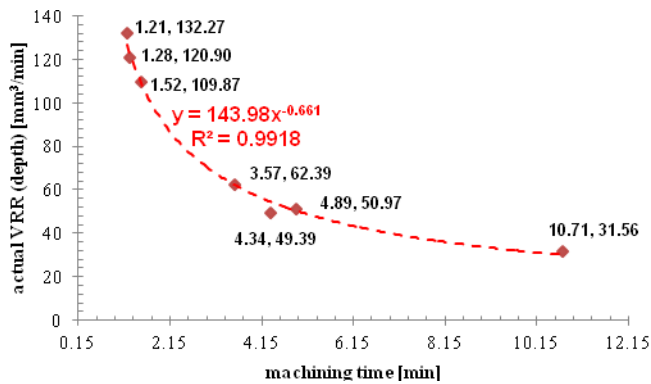


Figure 15 - Actual VRR (depth data) versus machining time, $U=const.$, $f \neq const.$

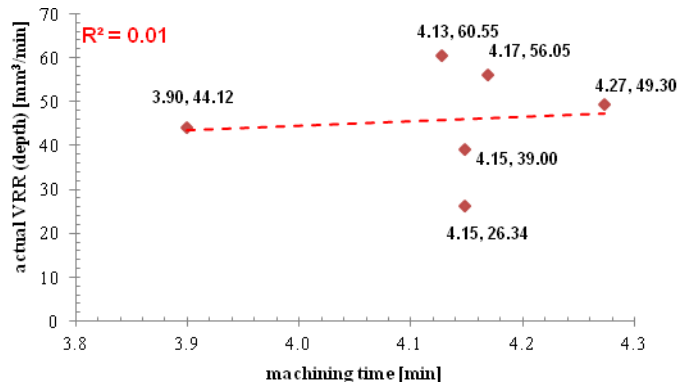


Figure 16 - Actual VRR (depth data) versus machining time, $U \neq const.$, $f=const.$

5.7. ACTUAL VOLUMETRIC REMOVAL RATE (FROM WEIGHT DATA)

$$V_w = \frac{\Delta m}{\rho \cdot t} \left[\frac{mm^3}{min} \right] \quad (8)$$

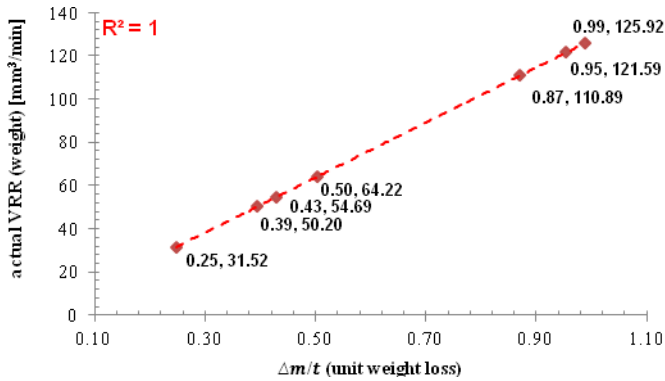


Figure 17 - Actual VRR (depth data) versus weight loss / unit time, U=const., f=const.

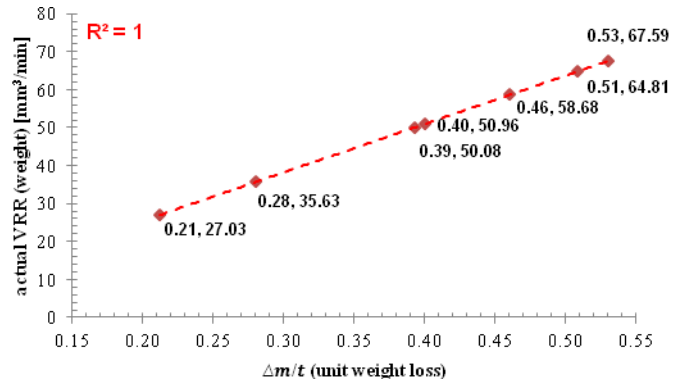


Figure 18 - Actual VRR (depth data) versus weight loss / unit time, U=const., f=const.

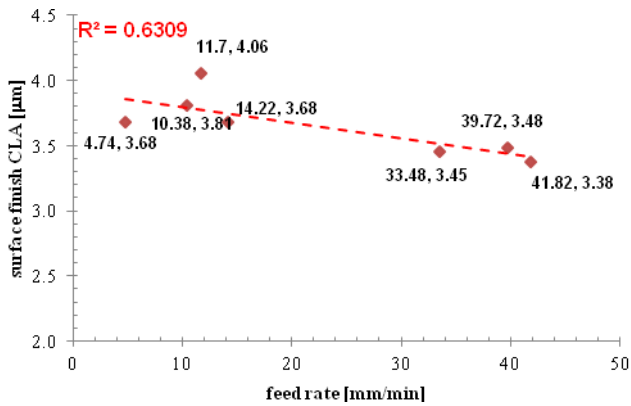


Figure 19 - Surface finish versus feed rate, U=const.

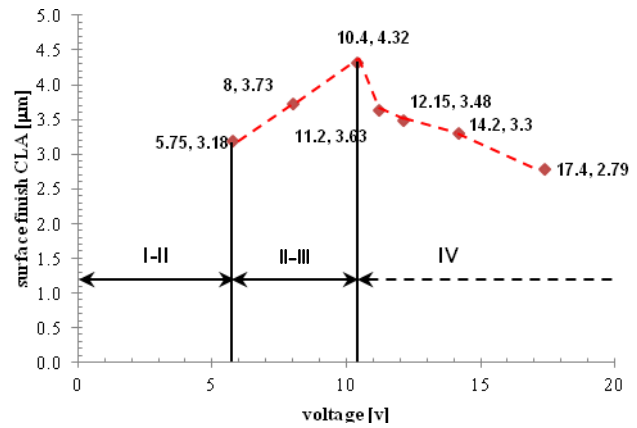


Figure 20 - Surface finish versus feed rate, U=const. [2]

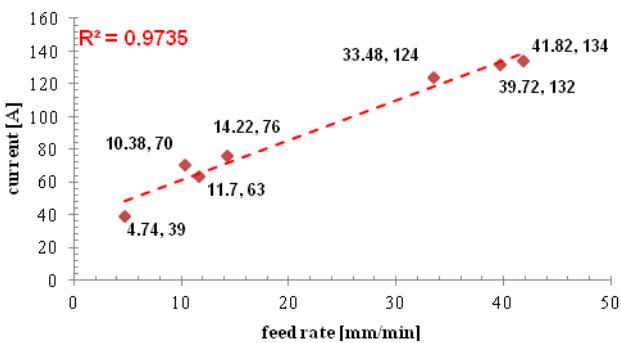


Figure 21 - Current versus feed rate

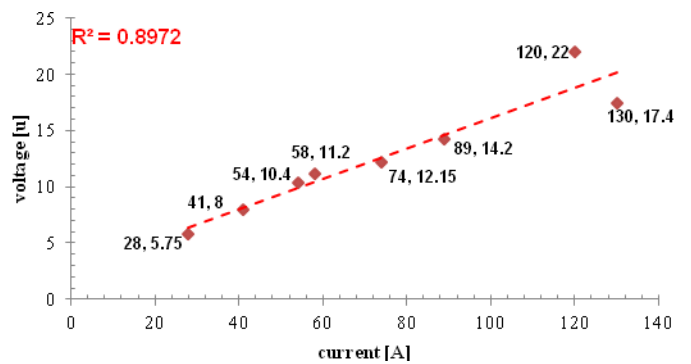


Figure 22 - Current versus Voltage

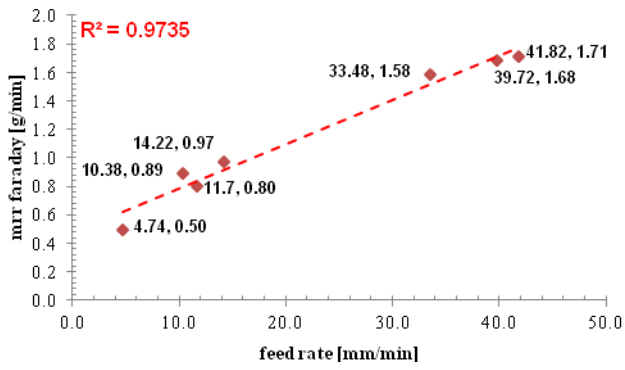


Figure 23 - Feed rate versus MRR according to Faraday, U=const.

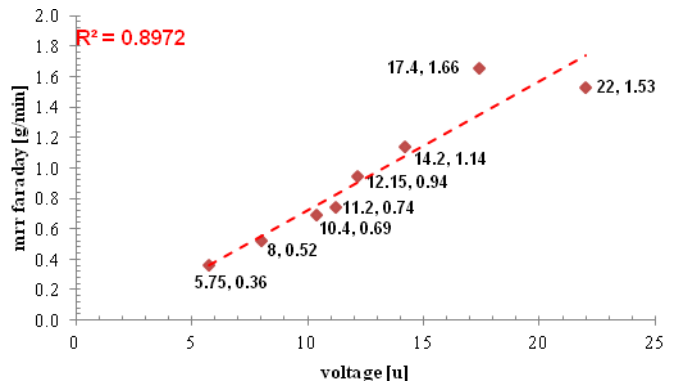


Figure 24 - Voltage versus MRR according to Faraday, U=const.

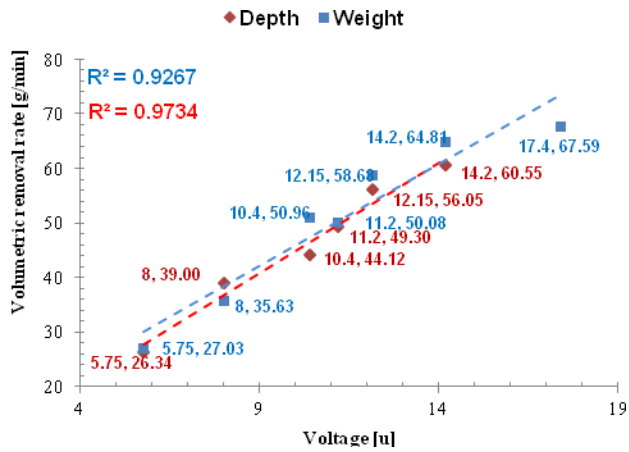


Figure 25 - Volumetric removal rates versus voltage, f=const.

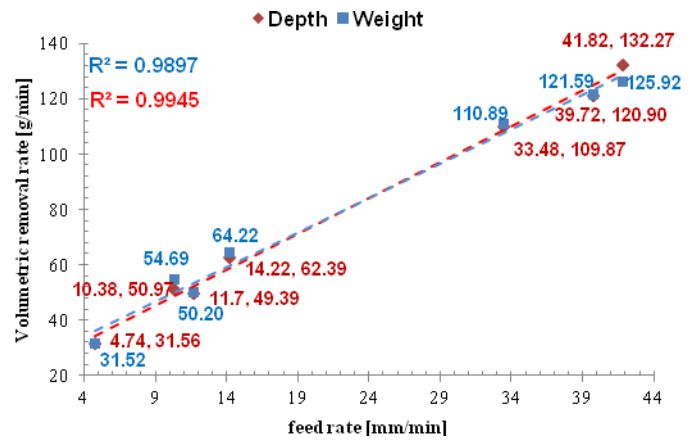


Figure 26 - Volumetric removal rates versus feed rate, U=const.

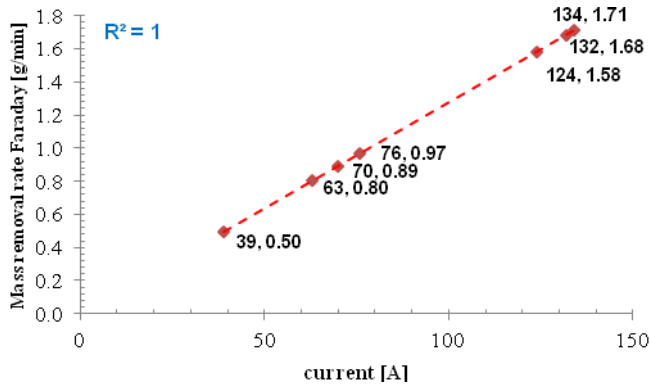


Figure 27 - Mass removal rate according to Faraday versus current, U=const.

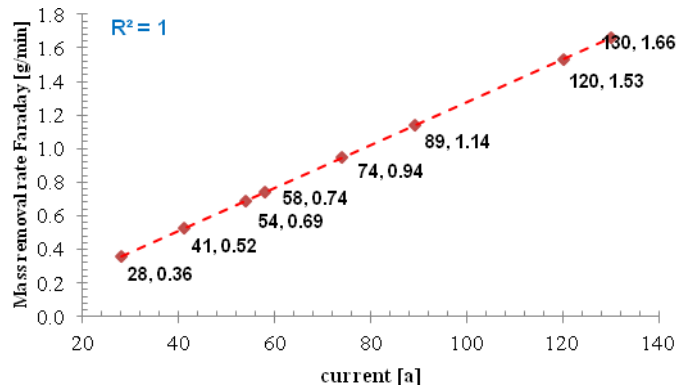


Figure 28 - Mass removal rate according to Faraday versus current, f=const.

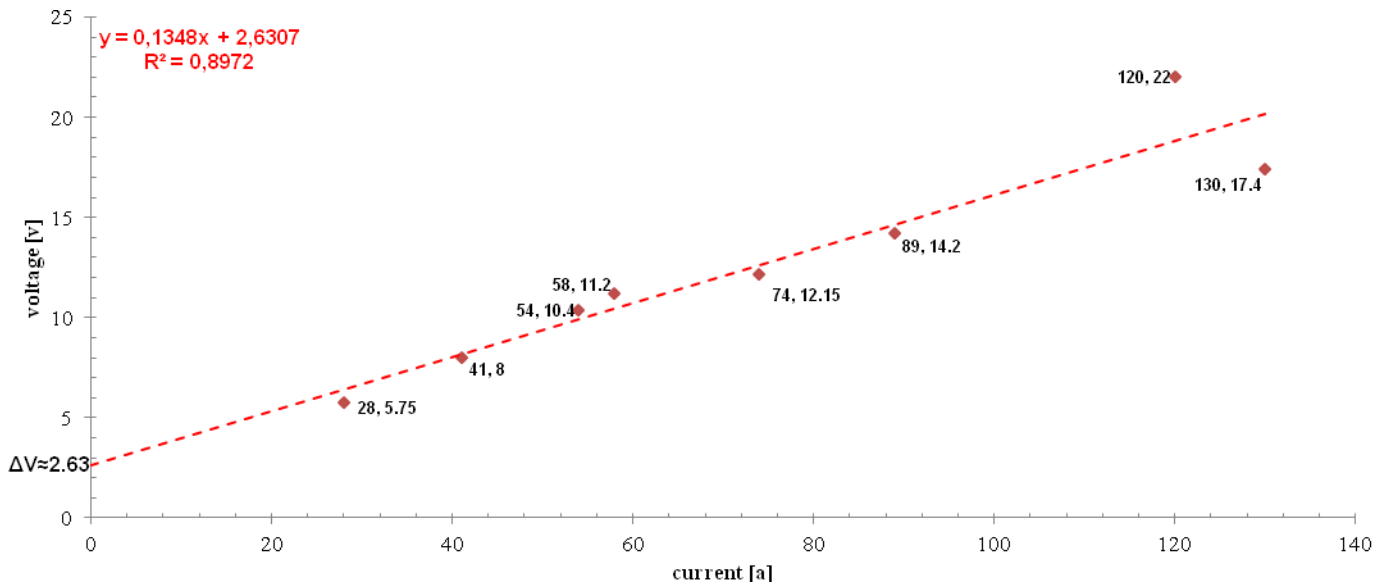


Figure 29 - Current versus voltage, $f = \text{const.}$ (at $I=0$, ΔV is the overpotential)

6. DISCUSSION OF RESULTS

Figures 7-29 depict the results according to the governing equations Eq.1-7. Two sets of data are distinguished; one set is at a constant voltage setting, the other at a constant feed rate. Since most of the results are fitted with linear regression or with the help of power-of- x functions and the goodness of fit is high, they are not discussed in detail here. Further analysis is required, however, for Figures 12, 16, 19, 20, 25, 26 and 29:

- **Figure 12:** Some sense of accuracy of the feed rate can be obtained from this graph. It can be seen that the scatter of the points is not widespread (ultimately, it should be one point for a constant feed setting), so it is safe to conclude that the feed was constant for the purpose of this experiment. An error of $\pm 2\%$ was expected.
- **Figure 16:** The points in this diagram are heavily scattered ($R^2 = 0.01$, a very bad fit for the linear regression). The linear relation between the actual volumetric removal rate from depth data cannot be assumed from the given data.
- **Figure 19:** The linear fit is somewhat off the optimal value ($R^2 = 0.63$) in the lower range of the feed rate. It can be seen, that at a given and constant voltage level, higher feed results in better surface finish.
- **Figure 20:** At a constant feed, the four process modes can clearly be established, and coincide with [2]:
 - I-II more MA and less ECD part
 - II-III more ECD, less ECD part
 - IV only ECD

- **Figure 25,26:** Both the weight- and depth-based volumetric removal rate data have a good linear fit with linear regression. The difference between the two methods is visibly negligible.
- **Figure 29:** Plotted at a constant feed rate, the voltage versus current diagram can be used to estimate the over-potential. When no current flows, the measured potential difference is the potential that is required to overcome all the different 'resistances' (activation-, reaction-, concentration-, bubble- and resistance overpotential) that do not follow from the expected values from thermodynamically determined reduction potential.

7. CONCLUSION

- the mass removal rate of the component increases with the voltage and the current;
- the MRR increases with the feed rate, but this results in a decrease of the final cut depth;
- surface roughness decreases with increasing feed rate
- a high feed rate decreases the equilibrium gap, resulting in a better surface finish and tighter tolerance;
- the VRR according to Faraday is roughly twice the amount calculated by the depth and the weight data (which correlate well with each other). This could be because of the efficiency factor of the electrolytic process. According to the data, $\eta \approx 50\%$ is expected. This seems reasonable according to Bannard J, who has investigated the effect of flow on steel during ECM and has found that –depending on the flow rate– the maximum current efficiency of NaNO_3 was maximum 70%.

8. REFERENCES

- [1] Abdel H, El-Hofy G, *Advanced machining processes: nontraditional and hybrid machining processes*, McGraw-Hill Mechanical Engineering Series (2005)
- [2] Atkinson J, *MACE61075 Advanced Manufacturing Processes Lecture notes*, The University of Manchester, (2011, Manchester)
- [3] Bannard J, *Effect of flow on the dissolution efficiency of mild steel during ECM*, Journal Of Applied Electrochemistry 7, pp. 267–270 (1977)

9. APPENDIX

Table 7 – Recorded data

SET DEPTH	FINAL DEPTH	FEED RATE	VOLTA GE	CURRENT	SURFACE FINISH	CHANGE IN WEIGHT	FLOW RATE GAUGE READING	TEMPERATURE	REMARKS
d_s [mm]	d_f [mm]	f [mm]	U [V]	I [A]	CLA [μ m]	Δm [g]	[l/s]	[°C]	-
CONSTANT VOLTAGE, VARIED FEED RATE									
0,11	0,36	11,7	13,8	63	4,06	1,71	21,2	19	-
0,16	0,37	14,22	13,8	76	3,68	1,8	21,5	19	SPARKS
0,14	0,56	4,74	13,85	39	3,68	2,65	21,1	19	-
0,14	0,28	33,48	13,8	124	3,45	1,32	21,1	19	SPARKS
0,14	0,26	39,72	13,65	132	3,48	1,22	21	20,50	SPARKS
0,14	0,27	41,82	13,75	134	3,38	1,2	21,3	20,50	SPARKS
0,14	0,41	10,38	13,8	70	3,81	2,1	21,2	20	-
CONSTANT FEED RATE, VARYING VOLTAGE									
0,13	0,29	13,02	10,4	54	4,32	1,56	21	19	FEW SPARKS
0,16	0,35	11,88	11,2	58	3,63	1,68	21,5	19	-
0,17	0,39	12,18	12,15	74	3,48	1,92	21,2	19,5	-
0,17	0,27	12,24	8	41	3,73	1,16	21,5	20	SPARKS
0,16	0,18	12,24	5,75	28	3,18	0,88	21,8	20	SPARKS
0,18	0,41	12,3	14,2	89	3,3	2,1	21,3	20	-
0,16	-	12,3	17,4	130	2,79	2,19	21,5	21	SPARKS
-	-	12,3	22,00	120	-	-	-	-	HEAVY SPARK, SHORT CIRCUIT, MACHINE STOPPED